ACRAMAN, SOUTH AUSTRALIA: AUSTRALIA'S LARGEST METEORITE IMPACT STRUCTURE

GEORGE E. WILLIAMS

Department of Geology and Geophysics, University of Adelaide, Adelaide, South Australia 5005

WILLIAMS, G. E., 1994:12:31. Acraman, South Australia: Australia's largest meteorite impact structure. *Proceedings of the Royal Society of Victoria* 106: 105–127. ISSN 0035-9211.

Acraman, located in the Mesoproterozoic Gawler Range Volcanics (1592±2 Ma) in the Gawler Ranges, South Australia, is the largest known impact structure in Australia. It is notable also as the source of an ejecta horizon of shocked volcanic fragments and melt material in Neoproterozoic (~590 Ma) shales in the Adelaide Geosyncline 220–350 km to the east and in coeval shales in the Officer Basin 470 km to the northwest of Acraman.

The centre of the structure is marked by sparse outcrops of shattered dacite in Lake Acraman within a topographic depression 30 km in diameter. The disrupted bedrock exhibits shatter cones and shock lamellae in quartz grains that indicate shock pressures of up to ~15 GPa. A partly fault-controlled apparent ring of valleys and low-lying country occurs at 85–90 km diameter, and satellite images reveal concentric arcuate features at ~150 km diameter.

Acraman is eroded below the original crater floor. The transient cavity that formed immediately after the impact was probably ~40 km in diameter and ~4 km deep. The central uplift of shock-deformed bedrock is ≥10 km in diameter. The structural rim of the 1.3-km-deep final collapse crater may be marked by the ring structure at 85–90 km diameter. Arcuate features at ~150 km diameter may be fractures marking the outer limit of disturbance.

The Acraman structure could have been formed by the impact of an Earth-crossing chondritic asteroid 4.7 km in diameter and of density 3500 kg/m^3 travelling at 25 km/s. The energy of crater formation was 6×10^{22} J, equivalent to 1.5×10^7 megatons of explosive energy. Ejecta blanketed at least 7×10^5 km^2. An Acraman-sized terrestrial impact of an Earth-crossing asteroid occurs on average every few tens of millions of years.

THE ACRAMAN STRUCTURE in South Australia (Fig. 1; Williams 1986, 1987, 1990) is Australia's largest known meteorite impact scar. Furthermore, Acraman is notable among known terrestrial impact structures in having parts of its widely dispersed distal ejecta-blanket of shattered rock preserved (Gostin et al. 1986).

The study of satellite images played a key role in my discovery of the Acraman structure. In 1979, while studying Landsat images for mineral exploration, I thought that the near-circular shape of Lake Acraman (latitude 32°01′S, longitude 135°26′E) and the surrounding topographic depression in the Gawler Ranges might record a major impact structure. In May 1980 I found intensely shattered Yardea Dacite, of the Mesoproterozoic Gawler Range Volcanics, on low islands within Lake Acraman. Petrographic study in 1980 showed that the shattered rocks contain quartz grains with shock lamellae, confirming an impact event. Although the structure was eroded below the former crater floor, it seemed likely that the crater had been at least 30 km in diameter, about the width of the topographic depression containing Lake Acraman. As such, Acraman was the largest impact structure known in Australia.

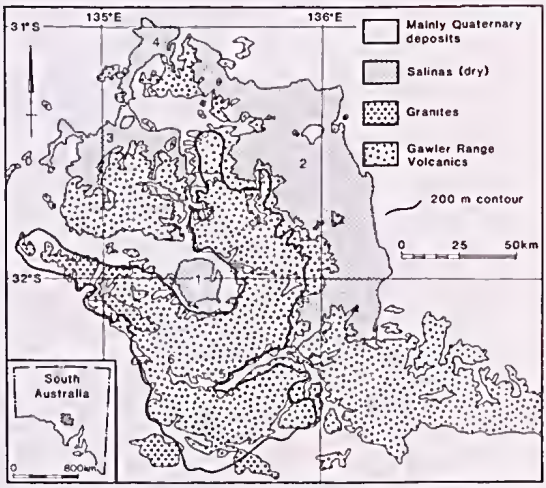

Fig. 1. Geological map of the Gawler Ranges region, South Australia, showing distribution of the Mesoproterozoic Gawler Range Volcanics and coeval granites. 1, Lake Acraman, within the Acraman depression; 2, Lake Gairdner; 3, Lake Everard; 4, Lake Harris; 5, the Yardea corridor, part of an apparent ring structure at 85–90 km diameter; 6, locality of strongly jointed Eucarro Dacite. The generalised 200-m contour is taken from the Port Augusta and Tarcoola topographic sheets (1 : 1 000 000).

In 1985, V. A. Gostin (University of Adelaide) told me of his discovery of volcanic rock fragments, interpreted as impact ejecta, in marine shales of the Neoproterozoic (~590 Ma) Bunyeroo Formation in the Flinders Ranges ~300 km east of Lake Acraman. Blocks of ejecta matched, both in general rock type and degree of shock metamorphism displayed, shattered rocks I had collected from Lake Acraman in 1980. Importantly, the connection between Acraman and the ejecta was indicated by U-Pb zircon ages of ejecta material determined by W. Compston and co-workers at the Australian National University. The wide extent of the ejecta horizon supported my conclusion that a major impact had occurred at Acraman; coarse ejecta must have fallen well beyond the western shore of the gulf-like Adelaide Geosyncline then occupying the position of the Flinders Ranges, to be preserved in muds on the sea floor.

NOAA satellite thermal infrared images of South Australia, newly available in 1985, showed Acraman as a conspicuous 'bullseye' ringed structure, with arcuate features at ~30, 85–90 and ~150 km diameter. The dimensions of the structure suggested that Acraman may rank with the largest impact structures recognised.

This paper reviews the geology and geophysics of the Acraman structure, and discusses the energetics and regional implications of the Neoproterozoic Acraman impact event.

REGIONAL GEOLOGY OF THE GAWLER RANGES

The Acraman impact structure (Fig. 1) lies almost entirely within the Gawler Range Volcanics, a Mesoproterozoic continental suite of mainly acid lavas and ash flows with an exposed thickness of 1 km in the Gawler Ranges (Rutland et al. 1981; Blissett 1986; Fanning et al. 1988; Giles 1988; Creaser & White 1991). The flat-lying, undeformed volcanics now cover more than 25 000 km^2 and outlying remnants indicate that formerly the suite was much more extensive. Gravity modelling suggests that the volcanics have a full thickness of ~4 km (Zhiqun Shi, pers. commun., 1992).

The Yardea Dacite, the uppermost and most widespread formation of the Gawler Range Volcanics (Creaser & White 1991), crops out continuously over 12 000 km^2; it has an exposed thickness of 250 m but probably is much thicker, and an unknown thickness has been removed by erosion. The Yardea Dacite is a highly porphyritic dacite grading to rhyodacite, with phenocrysts of plagioclase, alkali feldspar and hornblende typically 1–3 mm across, as well as augite, pigeonite and rare quartz, in a finely granular red brown or purplish brown microcrystalline matrix. An extensive 'black dacite' marks the base of the formation south of Lake Acraman. The Yardea Dacite shows remarkable mineralogical and geochemical homogeneity over its outcrop area, and ranks as one of the largest felsic volcanic units known.

Arcuate patterns as much as tens of kilometres across in the Gawler Range Volcanics, with volcanic units gently dipping inward, have been interpreted as evidence of cauldron subsidence or a caldera origin (Crawford 1963; Turner 1975; Giles 1977; Branch 1978; Rutland et al. 1981). However, Creaser & White (1991) suggested that no unequivocal evidence for volcanism of the 'caldera-collapse-resurgence' type is known from the Gawler Range Volcanics.

U-Pb zircon geochronology indicates an age of 1592 ± 3 Ma for the black Yardea Dacite and a pooled age of 1592 ± 2 Ma for extrusion of the Gawler Range Volcanics (Fanning et al. 1988). Granites of the Hiltaba Supersuite were intruded at 1585 ± 16 Ma (U-Pb zircon dating; Creaser 1989). The intrusion of the basic Gairdner dyke swarm commencing at 1050–1100 Ma was the last significant magmatic event in the Gawler Ranges region, and marks the earliest phase of rifting associated with the formation of the Adelaide Geosyncline (Parker et al. 1987).

Few earthquakes have been located in the Lake Acraman region, the International Seismological Centre listing only four small events within 90 km of Lake Acraman during 1964–1982. This low rate of seismic activity accords with the finding of Solomon & Duxbury (1987) that impact-induced faults do not long persist as lithospheric zones of weakness.

GEOMORPHOLOGY

Major geomorphological features of the Gawler Ranges region are revealed by digital elevation images (Fig. 2) and a map of the Lake Acraman area (Fig. 3).

The Lake Acraman salina (~20 km diameter, elevation 133–138 m) is eccentrically placed within a near-circular low-lying area 30 km across, termed here the 'Acraman depression' (140–200 m elevation). Except on the northwest, the depression is ringed by the Gawler Ranges that rise up to 300 m above the lake bed. This high ground, as outlined by the generalised 200 m contour (Fig. 1), forms an annulus 25–30 km wide that is breached in the northwest. The Gawler Ranges are bordered to the east and north by a low-lying area that contains the Lake Gairdner salina (113–121 m);

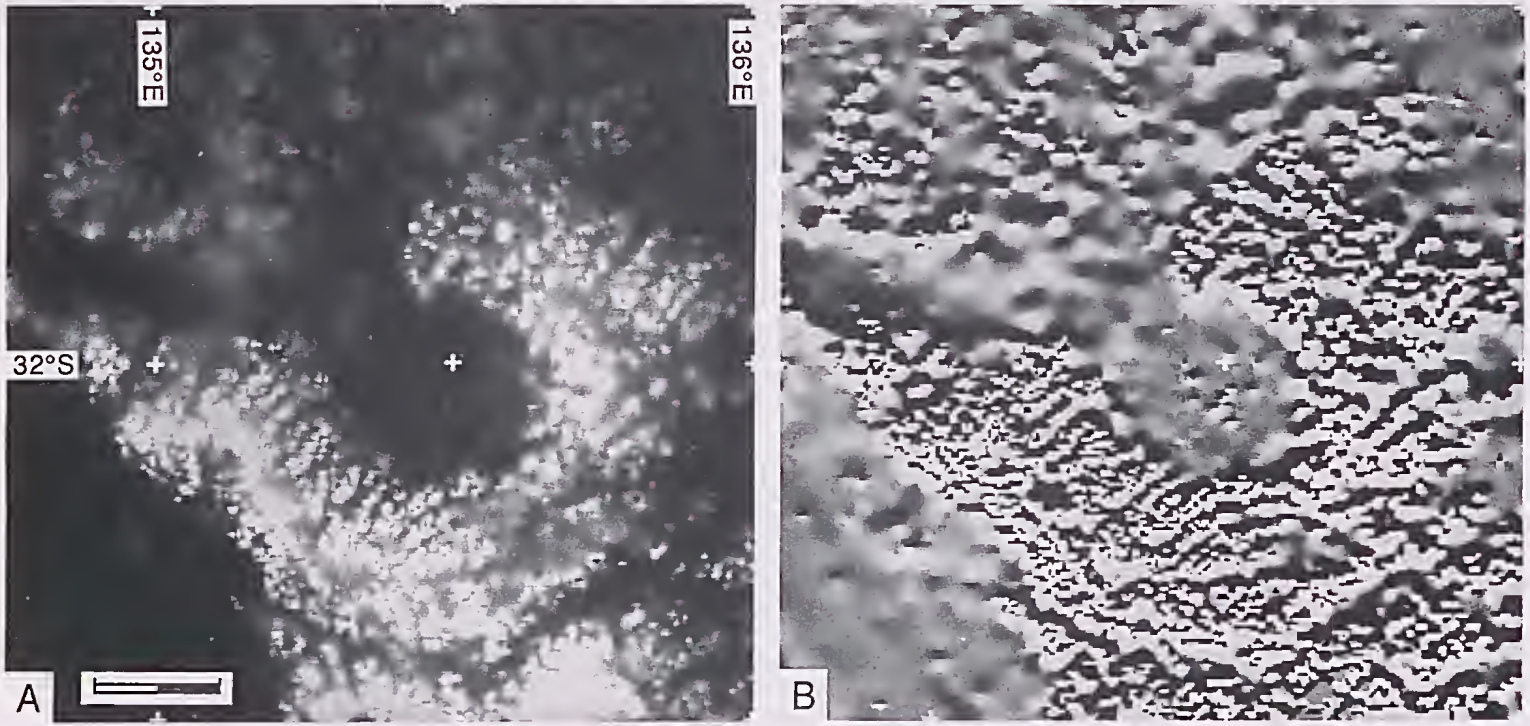

Fig. 2. Digital elevation images of the Gawler Ranges region, South Australia. (A) Grey scale image (light = high elevations, dark = low elevations) showing the Acraman depression surrounded by an annulus of elevated country, and the Yardea corridor at 85–90 km diameter. Scale bar 20 km. (B) Same area as (A) with gradients illuminated from the south, showing a cluster of small peaks near the centre of the Acraman depression, and the Yardea corridor. Images derived from data supplied by the Australian Surveying and Land Information Group and reproduced with the permission of the General Manager, AUSLIG, Department of Administrative Services, Canberra. Data processed by BHP Minerals Exploration Department, Melbourne.

Fig. 3. Geological map of the Aeraman depression (=inner topographie depression of the Aeraman structure), showing: the outcrop pattern of Yardea Daeite and granite in the Gawler Ranges; the general distribution of Quaternary lacustrine, aeolian and alluvial deposits; field localities, with numbers; and the position of the dipolar aeromagnetic anomaly in the central area of Aeraman (cross). Modified from Blissett (1977) and Blissett et al. (1988), with outcrops of Yardea Daeite within Lake Acraman mapped by the present author. To protect rock outcrops, the area of the Acraman depression has been declared a Geological Monument of the Geological Society of Australia, and the Aeraman structure is on the Indicative List of Australian sites for inclusion in the UNESCO Global Inventory of Geological and Fossil Sites.

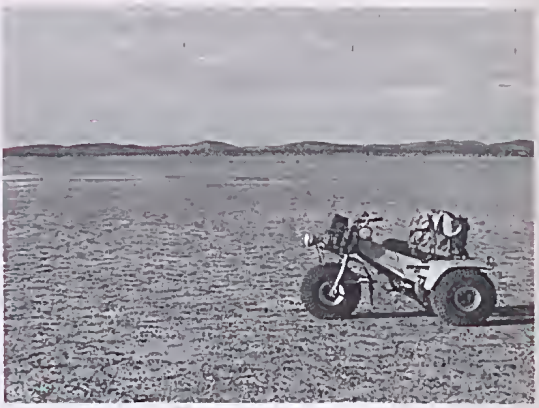

Fig. 4. View looking south across the dry bed of Lake Aeraman, with the Gawler Ranges on the skyline.

low country that includes the Lake Everard and Lake Harris salinas (121–124 m) lies to the northwest. The Gawler Ranges are flanked on the south and west by subdued terrain (90–200 m) marked by seif dunes and scattered small salinas.

The topography reflects the strong influence of structure sculptured by several cycles of erosion since Mesozoic time. A high-level summit surface of Cretaceous age—the Nott Surface (Twidale et al. 1976)—has elevations of 430–450 m south of Lake Acraman and 300–330 m north of that lake. The surface was initiated by weathering of a peneplain in Jurassic time; stripping of the regolith and formation of the Nott Surface as a high-level etch surface were caused by northward tilting of the peneplain during the Early Cretaceous (Campbell & Twidale 1991). The Nott Surface is now dissected to depths as great as 250 m below summit levels in the Gawler Ranges south of Lake Acraman and to a depth of 150 m north of the lake.

The surface of the Acraman depression (Fig. 3) slopes gently inward from an elevation of 180–200 m at the base of the surrounding ranges to 140 m near the margin of Lake Acraman. The depression is underlain by weathered Yardea Dacite mantled by Miocene–?Early Pliocene ferruginous and siliceous duricrusts as well as by Pleistocene and Holocene alluvium and colluvium (see Blissett et al. 1988). This duricrusted plain formed during the Tertiary and may be compared to Tertiary surfaces that floor valleys elsewhere in the Gawler Ranges (see Twidale et al. 1976). During the Tertiary, drainage found an outlet via the low-lying country (≲150 m elevation) northwest of Lake Acraman and thence northward along a palaeodrainage course now marked by the Lake Everard–Lake Harris chain of salinas (Fig. 1).

The bed of Lake Acraman is as much as 6 m below the level of the adjacent plain; the distant ranges surrounding the lake on most sides (Fig. 4) give the impression of a vast amphitheatre. Like other salinas in southern Australia, Lake Acraman developed by aeolian deflation during Pleistocene arid intervals (see Bowler 1986). The lake is now a closed basin where saline ground waters crop out, and is floored by damp, sulphidic clays usually veneered by a thin (millimetre) crust of sodium chloride. Under the action of prevailing westerly winds during the Pleistocene, clay, quartz sand and fine-grained gypsum from the lake bed were built into a series of mainly gypseous dunes rising to 30 m above the lake bed on the upwind (western and northwestern) margins of islands. An arcuate bordering dune or lunette rising to 25 m above the lake bed also was built at the eastern and south-

eastern margin of the lake. Low outcrops of intensely shattered dacite are restricted to the lee (eastern) side of several islands in the southeastern part of Lake Acraman near the centre of the Acraman depression.

Dissection of the Nott Surface has been strongly influenced by joints and structural lineaments in the Gawler Range Volcanics (Fig. 5). The dominant regional trend of joint-controlled valleys in the Yardea Dacite is northeast, with other trends between north and northwest. In addition, several linear structural 'corridors' 3–10 km wide, marked by subdued outcrop and small depressions with salinas, traverse the Gawler Ranges region (Fig. 5). The intersection of two lineaments with the palaeodrainage outlet northwest of Lake Acraman accounts for the paucity of outcrop in that area. The joint and fracture patterns in the volcanics evidently are of great antiquity, having influenced the form of a palaeosurface buried by Mesoproterozoic (1400 Ma) sandstones in the eastern Gawler Ranges (Campbell & Twidale 1991). The Gairdner dyke swarm parallels the northwest-trending fractures.

The 'Yardea corridor' (Williams 1986) 30 km south of the Acraman depression comprises several near-linear valleys as much as 3 km wide that together extend for at least 70 km roughly concentric with the southern margin of the depression (Figs 1 and 2). A fault follows the Yardea corridor for 35 km (Blissett 1987; Blissett et al. 1988), but the history of movement on the fault is unknown.

SATELLITE IMAGES OF THE ACRAMAN STRUCTURE

The Acraman structure is clearly revealed by visible spectrum and infrared satellite images. In particular, satellite infrared images, by distinguishing small differences in surface temperature, can highlight regional structures such as faults, fractures and palaeodrainage courses that are not readily seen on visible spectrum images and photographs.

A Landsat image of most of the Acraman structure (Fig. 5) shows an inner depression (the Acraman depression) and part of an intermediate 'ring' stucture, which includes the Yardea corridor, at 85–90 km diameter. An arcuate feature also is evident at ~150 km diameter, extending 170 km from the southeastern corner of Lake Gairdner northwestward to Lake Everard. West of this feature the bed of Lake Gairdner appears to be crossed by numerous shallow channels containing surface water, in contrast to the dry lake bed to the east. Drilling in Lake Gairdner (Johns 1968) revealed a salt crust as much as 450 mm thick and abundant halite and gypsum in lake sediments to depths of 14 m west of the arc, but only silt at least 3 m thick with no salt crust to the east. Johns (p. 74) noted that the salt crust 'thinned abruptly' eastward from a locality near the arc. The apparent change in character of the lake deposits across the arc through Lake Gairdner suggests that the line may follow basement faults or buried topography, with generally deeper bedrock to the west. Geophysical studies might test these interpretations.

A NOAA-AVHRR (National Oceanographic and Atmospheric Administration Advanced Very High Resolution Radiometer) satellite thermal infrared night image of northern South Australia (Fig. 6) reveals Acraman as a conspicuous ringed structure. The inner depression is largely encircled by the intermediate 'ring' at 85–90 km diameter; these features appear cooler (darker) possibly because of greater vegetative cover promoted by higher soil moisture. This ring comprises several near-linear features 30–40 km long that together produce a polygonal outline. A break in the ring occurs northwest of Lake Acraman where other lineaments coincide with the palaeodrainage outlet; the palaeodrainage line may be influenced by a north-trending structure. Arcuate features at ~150 km diameter include a line running through lakes Gairdner and Everard, and possibly the southern limit of the Gawler Ranges south of Lake Acraman. The NOAA image also shows several lineaments unrelated to the Acraman structure.

Hence, satellite images support topographic evidence (Figs 1 and 2) that the main geomorphological elements of the Gawler Ranges are centred on the Acraman depression. This regional arrangement is unrelated to the stratigraphy of the Gawler Range Volcanics.

SHATTERING AND SHOCK METAMORPHISM

Shattered rocks in the central area

Good outcrop of intensely shattered and shocked Yardea Dacite occurs at three localities (Fig. 3, locs 3, 12, 15) on two islands in the southeastern part of Lake Acraman near the centre of the Acraman depression. Poor outcrop of shattered dacite occurs at localities 13 and 14.

The better outcrops display several fracture patterns. Typically the dacite contains numerous closely spaced (millimetre to centimetre), randomly-oriented fractures that produce an irregular mosaic of rock fragments (Fig. 7A). Intense shattering


0
30 km
1
2
2
3
4
5

locally has produced a breccia of finely crushed dacite that may contain fragments of less fractured rock (Fig. 7B).

Near-parallel fractures up to 50 mm apart locally produce platy fragments arranged roughly perpendicular to shallow-dipping joints in the dacite. A reticulate fracture pattern is produced over small areas by groups of near-perpendicular fracture planes 10–20 mm apart.

Broken surfaces of disrupted dacite commonly display striae that locally form small shatter cones (Fig. 7C). Larger shatter cones up to 150 mm long also occur, but are too few to provide reliable structural data. The shatter cones are not as well formed as those developed in fine-grained sedimentary rocks in other impact structures (e.g. Milton 1977).

Fractured rocks outside the central area

Outcrops of fractured Yardea Dacite occur at the margins of islands near the northern and western shores of Lake Acraman (Fig. 3, locs 17, 18). The fracturing does not approach the intensity of disruption in the central area, and shatter cones have not been observed.

Rocks outside the Acraman depression in general are not unusually fractured and shatter cones have not been observed. Isolated outcrops of Yardea Dacite within the Yardea corridor display numerous closely spaced (~ 50 mm) near-vertical joints which strike northwest obliquely across the trend of the corridor. The jointing may reflect fault movement at the corridor margin.

Outcrop of Eucarro Dacite stratigraphically below the Yardea Dacite 23 km northwest of Yardea Homestead (Fig. 1) is strongly jointed and has variable magnetic properties (Blissett et al. 1989). Joints are closely spaced ($\lesssim$10 mm) and display near-horizontal and near-vertical attitudes. Near-vertical joints locally produce a reticulate pattern like that in the central area of Acraman. Curved joint sets also are present, but shatter cones have not been observed. These disturbed rocks occur near the intermediate ring structure at 85–90 km diameter.

Petrography of the shattered rocks

Yardea Dacite from the central area contains phenocrysts of plagioclase and very minor K-feldspar up to 3 mm long in a fine-grained matrix of K-feldspar intergrown with granular to myrmekitic quartz. Finely divided iron oxide gives the feldspars a red brown colour.

All the shattered rocks studied show microscopic evidence of fracturing and deformation. The fractures, which occur in feldspar phenocrysts and matrix, are defined by limonite-lined veinlets and zones of clear, recrystallised felsic minerals. Several wider fractures contain irregular voids partly lined with clear authigenic feldspar. Some feldspar phenocrysts in the more strongly deformed rocks have highly fractured and deformed shapes showing localised granulation and microbreccia textures. Zircon and apatite grains are greatly fractured. A brown micaceous mineral identified by XRD as stilpnomelane occurs on some fracture surfaces.

From 5–90% of quartz grains in thin-sections of shattered dacite from localities 3 and 15 and rare quartz grains in specimens from locality 12 exhibit closely spaced, parallel planar lamellae, decorated with cavities and finely divided material, that do not transgress grain boundaries (Fig. 7D). As many as four different sets of lamellae have been observed in the same grain. These planar features are identical to the shock lamellae developed in quartz grains in impactites (Robertson et al. 1968). The attitudes of 54 sets of lamellae seen in thin sections of two samples from locality 3, and measured with a universal stage, indicate $\omega\{10\bar{1}3\}$ (dominant) and $\xi\{11\bar{2}2\}$ crystallographic orientations, and a high-angle set (70–80°) that may be $\Upsilon\{40\bar{4}1\}$ (Fig. 8). Lamellae densities range from 300–600 per millimetre. These features indicate Type C shock deformation of Robertson et al. (1968) and shock pressures of ~15 GPa (see Robertson & Grieve 1977). Closely spaced shock lamellae in one or more sets occur also in some feldspars in the shattered dacite.

Because of the paucity of outcrop in Lake Acraman and the surrounding depression, the true dimensions of the central area of intense shattering and shock metamorphism cannot be determined,

Fig. 5. Landsat image covering most of the Acraman structure, showing: 1, Lake Acraman within the Acraman depression; 2, Lake Gairdner; 3, Lake Everard; 4, the Yardea corridor at 85–90 km diameter. Surface water (darker areas) in Lake Gairdner helps define an arcuate trend (5) that continues westward to Lake Everard and may mark the outer limit of disturbance at ~150 km diameter. The Gawler Range Volcanics shows strong jointing, and a northwest-trending structural lineament occurs on the northern side of Lake Acraman. A Tertiary palaeodrainage course runs northward from the northwestern margin of the Acraman depression via a chain of small salinas and Lake Everard. Landsat scene 15 February 1973, scene centre S31-30 E135-51; processed by BHP Minerals Exploration Department, Melbourne.

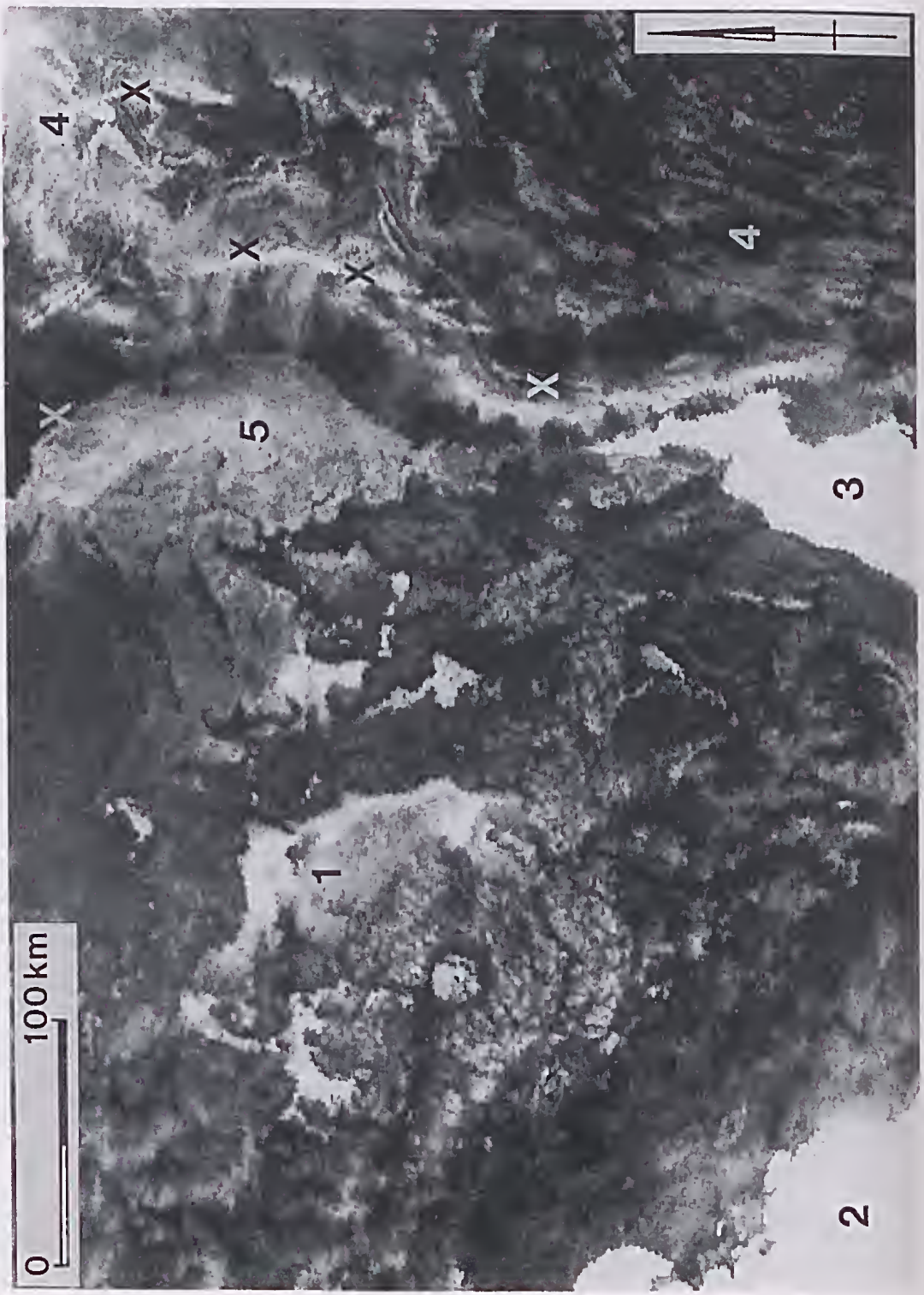
0
100 km
1
2
3
4
4
5

but a minimum diameter of 10 km is suggested by the sparse outcrop. Rocks outside the central area show little if any microscopic evidence of fracturing or deformation, and shock lamellae have not been observed in quartz or feldspar grains.

IMPACT MELT

Outcrop of melt rock (basement rock melted by the impact) at locality 15 in the central area appears to be part of a gently-dipping dyke 1.5 m thick that occurs along a strike length of ~300 m. The melt rock is aphanitic and usually red brown in colour, weathering to buff hues, and is unshattered. Inclusions of dacite range from small xenocrysts of feldspar and partly resorbed xenoliths to blocks of shattered rock as much as 200 mm across; overall, however, the melt rock contains <15% inclusions. The contact with the dacite is marked by irregular-shaped, partly resorbed dacite xenoliths (Fig. 7E) or intensely shattered dacite microbreccia.

Petrography, and XRD and electron-microprobe analyses show that the melt rock consists mainly of slender, twinned, skeletal laths of albite as large as 350×20 μm and commonly arranged in radial quench textures, set in a matrix of cloudy K-feldspar and finely intergrown quartz (Fig. 7F). The matrix also contains finely dispersed iron oxide, as well as scattered larger euhedral grains of variably oxidised titaniferous magnetite up to 30 μm in diameter. Partly resorbed xenoliths comprise microcrystalline aggregates of quartz, K-feldspar and fine-grained cloudy material, and commonly have a reaction rim of titaniferous magnetite grains. Rare corroded quartz xenocrysts display single or multiple sets of shock lamellae.

Microprobe analyses indicate that the Na- and K-feldspar phases in the melt rock have virtually pure, end-member compositions (Ab_{99} and Or_{98}; Table 1). Such compositions indicate that they are low-temperature feldspars (see Kastner & Siever 1979; Boles 1982) formed by secondary alteration of the melt rock, rather than high-temperature equilibrium products of a melt derived from the Gawler Range Volcanics (see Carmichael et al. 1974). The albite laths are the result of low-temperature albitisation of a primary high-temperature feldspar. The matrix K-feldspar and finely intergrown quartz may be devitrification products of glassy material.

The fine-grained, generally inclusion-poor nature of the melt rock, the characteristic quench textures, the presence of shocked-deformed inclusions of quartz, and its limited outcrop within the central area of intensely shattered rocks are all consistent with the melt rock being a dyke or sill below the crater floor (see Dence 1971; Grieve et al. 1977). There is no geological or aeromagnetic evidence that the melt rock represents part of a widespread melt pool in an annulus around a central uplift.

GEOCHEMISTRY

Analyses of undisturbed Yardea Dacite from many localities in the Gawler Ranges, and of shattered Yardea Dacite, dacite microbreccia, and melt rock from the central area at Acraman, are given in Table 2. The Yardea Dacite has a remarkably uniform composition over much of its area, most samples containing from 66% to 69% SiO_2 (Creaser & White 1991). No important difference between the undisturbed and shattered dacite is evident in Table 2; the greater CaO content and LOI for the shattered rocks may indicate their minor secondary alteration.

The three specimens of melt rock assayed show very limited compositional range and have some similarity to the composition of the Yardea Dacite. Apparent trends exist for several elements in the sequence from undisturbed and shattered dacite, through microbreccia, to melt rock. Most notable is the 40–50% increase in potassium content of the melt rock; conversely, the melt rock is depleted slightly in total Fe, MgO and CaO compared with the undisturbed and shattered dacite. Enrichment in potassium and increase in K_2O/Na_2O ratio in melt rock relative to country rock have been observed at other impact sites (Dence 1971; Hartung et al. 1971; Parfenova & Yakovlev 1977; Grieve 1987). A favoured explanation of such potassic enrichment is hydrothermal alteration, particularly

Fig. 6. Thermal infrared night image of northern South Australia taken by NOAA satellite. Warm areas including the sea and some salinas appear white, cool areas dark. The Acraman structure appears as a large ringed feature in the western part of the scene, comprising a dark, circular inner area (inner depression) that contains Lake Acraman (paler tone) and concentric features at 85–90 km (dark, polygonal ring) and ~150 km diameter; the ring structure is breached on the northwest by northwest- and north-trending lineaments. Geographic features include: 1, Lake Gairdner; 2, Great Australian Bight; 3, Spencer Gulf; 4, Flinders Ranges; 5, Lake Torrens. Crosses mark main ejecta localities in the Flinders Ranges (northern Adelaide Geosyncline) as much as 350 km from Acraman. NOAA9-AVHRR Band 3, Orbit no. 2246, 21 May 1985, 2200 hours. Image geometrically corrected, Lambert conic conformal projection; processed by BHP Minerals Exploration Department, Melbourne.

of highly shocked felsic clasts, during the impact event.

No important difference exists among trace element values for undisturbed Yardea Dacite, shattered dacite, and melt rock. The values usually do not exceed average abundances for the Earth's crust or acid igneous rocks (see Levinson 1974), although values for Zr, Ba and rare earth elements (La, Ce, Nd) tend to be elevated. A trace element spidergram for undisturbed Yardea Dacite from numerous localities is shown in Fig. 9.

Values for Cr, Co, Ni and platinum-group

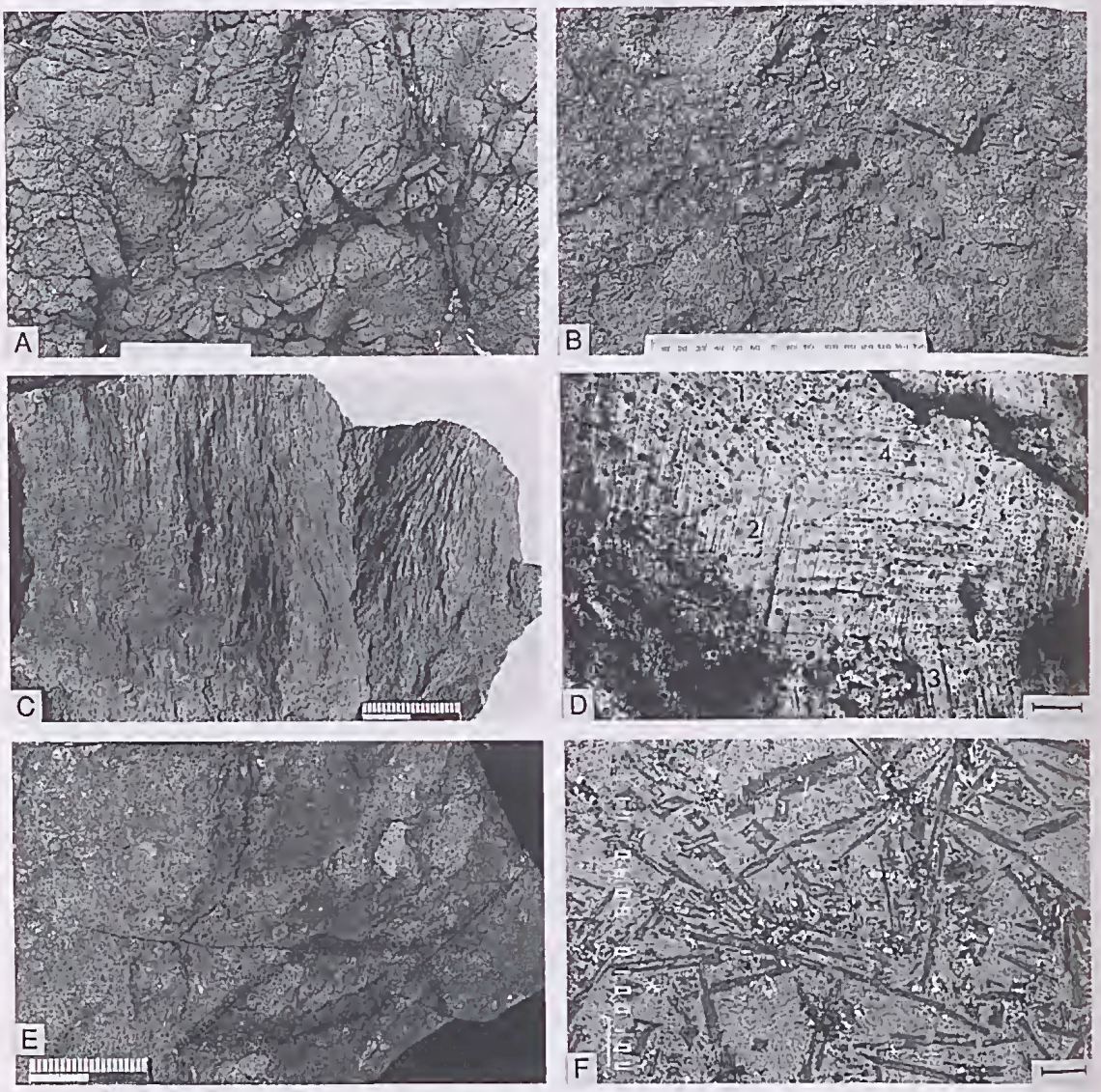

Fig. 7. (A) Strongly fractured Yardea Dacite bedrock, locality 12; scale 150 mm. (B) Brecciated Yardea Dacite, locality 12; scale 150 mm. (C) Broken surface of disrupted Yardea Dacite showing striae and small shatter cone, locality 3; scale 20 mm. (D) Four sets of decorated shock lamellae in a quartz grain from disrupted Yardea Dacite, locality 3; crossed polars, scale bar 25 μm. Sets 1, 2 and 3 parallel to ω crystallographic orientation and set 4 probably parallel to T. (E) Disrupted Yardea Dacite (left) and melt rock (darker rock on right), with partly resorbed xenoliths of dacite at the contact, locality 15; scale 20 mm. (F) Electron probe photomicrograph of melt rock from locality 15, showing skeletal laths of albite in a devitrified matrix of K-feldspar (pale) and quartz (darker flecks); scattered grains of iron oxide appear white, black spots are voids. Scale bar 100 μm.

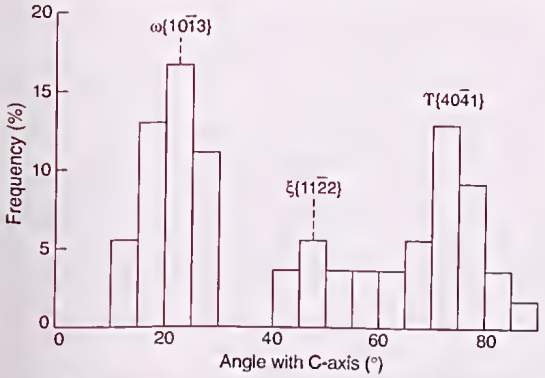

Fig. 8. Frequency histogram for the angle (in degrees) between the *c*-axis and the pole of 54 sets of shock lamellae in quartz grains in shattered Yardea Dacite, locality 3, central Acraman structure. Crystallographic orientations typical of Type C shock deformation (shock pressures ~15 GPa) in shock-deformed quartz are shown.

	Laths (21)	Matrix (17)	Xenoliths (2)
SiO_2	69.73 ± 0.38	66.14 ± 0.79	67.29
Al_2O_3	19.44 ± 0.17	17.86 ± 0.42	16.99
K_2O	0.12 ± 0.05	15.57 ± 0.53	14.98
Na_2O	10.53 ± 0.50	0.32 ± 0.19	0.47
CaO	0.09 ± 0.08	–	–
MgO	0.03	–	0.20
FeO	0.04	0.12	–
Cl	0.01	–	–

Table 1. Electron microprobe analyses of feldspar phases in melt rock from locality 15, central Acraman structure. Values shown are means (with ±1σ where applicable) obtained from analyses summed to 100%. Number of analyses in brackets. JEOL 733 Microprobe facility, Electron Optical Centre, University of Adelaide.

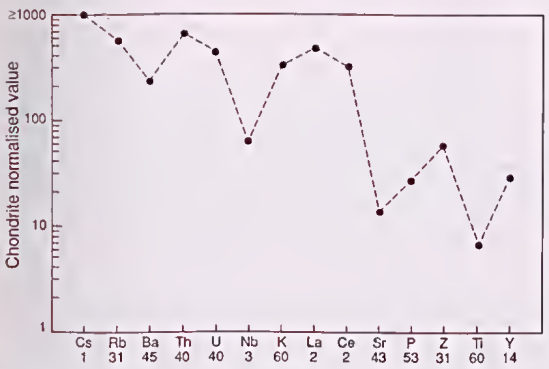

Fig. 9. Trace element spidergram for the Yardea Dacite from numerous localities; the figures below the elements give number of analyses. After Blissett et al. (1989).

elements (PGEs) for shattered dacite and melt rock are not significantly different from values for undisturbed Yardea Dacite. All samples assayed have negligible PGE values. Rocks from several other major impact structures likewise show no anomalous Cr, Co, Ni (Currie & Shafiquallah 1968) and Ir (Palme 1982). The lack of anomalous cosmogenic siderophile elements in the shattered dacite and melt rock at Acraman may reflect erosion to a level well below the former crater floor.

GEOPHYSICAL SIGNATURE

Gravity

The Bouguer gravity anomaly signature for the Gawler Ranges region (Fig. 10) is dominated by several positive anomalies that together form a broad gravity high of amplitude ~20 mGal and 150×100 km in extent that approximates the main area of outcrop of the Gawler Range Volcanics. This broad positive anomaly may reflect more dense, basic rocks at a depth between ~4 and ~12 km (D. Boyd & Zhiqun Shi, pers. commun., 1992).

Most structural and topographic features within the Gawler Ranges cannot be related to the Bouguer gravity signature. The notable exception is the Acraman depression, which is covered by a near-circular negative anomaly of ~6 mGal amplitude and 30–35 km in diameter within a broader gravity low (as much as 10–15 mGal amplitude and ~50 km across). The arcuate features at 85–90 and ~150 km diameter appear unrelated to the regional gravity signature.

Near-circular negative gravity anomalies commonly are associated with impact structures (Pilkington & Grieve 1992), reflecting fractured and brecciated material of lower density than the surrounding undisturbed rocks. No central gravity high such as are displayed by some large impact structures has been identified at Acraman, although the wide gravity-station spacing usually of 5 to 8 km does not permit detailed resolution of the gravity signature.

Density differences between hand specimens of undisturbed Yardea Dacite (mean density 2660 kg/m^3) and shattered dacite from the centre of Acraman range from 0 to 150 kg/m^3, and between undisturbed Yardea Dacite and melt rock from 160 to 240 kg/m^3. Precise modelling of the negative gravity anomaly over Acraman is limited by the wide station spacing, but the anomaly is consistent with disrupted material extending to a depth of at least 5 km beneath the Acraman depression, possibly into underlying denser rocks (Zhiqun Shi, pers. commun., 1992).

	Yardea Dacite*	Yardea Dacite†	Shattered Yardea Dacite§	Microbrecciated Yardea Dacite**	Melt rock††
SiO_2 (%)	67.69 (60)	67.8 (2)	66.1 (3)	70.4	68.6 (3)
TiO_2	0.70 (60)	0.67 (2)	0.76 (3)	0.83	0.83 (3)
Al_2O_3	13.68 (60)	13.5 (2)	13.4 (3)	12.7	14.6 (3)
Fe_2O_3§§	3.18 (59)	5.02 (2)	5.18 (3)	3.13	2.53 (3)
FeO	2.90 (38)	–	–	–	–
MnO	0.16 (60)	0.12 (2)	0.23 (3)	0.03	0.03 (3)
MgO	1.12 (60)	0.91 (2)	0.73 (3)	0.46	0.36 (3)
CaO	1.66 (60)	1.32 (2)	2.99 (3)	0.29	0.29 (3)
Na_2O	2.95 (60)	3.01 (2)	3.72 (3)	2.27	2.85 (3)
K_2O	4.98 (60)	5.27 (2)	4.65 (3)	6.75	7.30 (3)
P_2O_5	0.28 (53)	0.17 (2)	0.17 (3)	0.25	0.19 (3)
LOI	1.21 (20)	1.90 (2)	2.63 (3)	2.05	2.55 (3)
Cr (ppm)	29 (41)	47 (2)	73 (4)	72	58 (3)
Co	15 (41)	7 (2)	9 (5)	6	6 (3)
Ni	12 (39)	6 (2)	10 (4)	8	5 (2)
Cu	22 (41)	16 (2)	28 (5)	5	10 (3)
Zn	97 (41)	96 (2)	86 (5)	22	26 (3)
Pb	52 (38)	12 (2)	25 (5)	22	20 (3)
V	38 (43)	19	39	–	–
Rb	205 (31)	200 (2)	188 (4)	180	182 (3)
Sr	160 (43)	145 (2)	195 (4)	270	317 (3)
Ba	1631 (45)	1360 (2)	1254 (5)	1840	817 (3)
Zr	406 (31)	417 (2)	373 (4)	420	433 (3)
Nb	22 (3)	23 (2)	20 (4)	22	23 (3)
U	6 (40)	–	–	–	–
Th	28 (40)	28	25	–	–
Ga	–	20	18	–	–
Sc	13 (2)	10	12	<20	<20 (3)
Y	55 (14)	60 (2)	38 (5)	26	24 (3)
La	79 (2)	80	78 (4)	110	130 (3)
Ce	142 (2)	148 (2)	110 (5)	120	177 (3)
Nd	–	60 (2)	57 (4)	<20	63 (3)
Pd*** (ppb)	–	0.78	0.61	–	0.31 (3)
Pt	–	0.84	0.62	–	1.03 (3)
Au	–	0.19	0.14	–	0.13 (3)
Ir	–	<0.005	<0.005	–	0.01 (3)
Ru	–	–	–	–	0.11 (3)

Table 2. Whole rock analytical data for Yardea Dacite, and shattered dacite and melt rock from the Acraman impact structure. (*Note:* Where mean values are given, the number of samples analysed is shown in brackets.) *Undisturbed Yardea Dacite from all areas; data from Blissett et al. (1989). †Undisturbed Yardea Dacite from locality 21, 6 km west of Lake Acraman (see Fig. 3). One sample analysed by Classic Comlabs, Adelaide, using XRF and wet chemistry. Values for other sample by courtesy of M. W. Wallace, R. R. Keays and V. A. Gostin. §Samples from localities 3, 12 and 15, central area of Acraman, analysed by Classic Comlabs, Adelaide, using XRF and wet chemistry. Additional trace element and PGE values for one sample from locality 12, by courtesy of M. W. Wallace, R. R. Keays and V. A. Gostin. **Sample from locality 15, analysed by Classic Comlabs, Adelaide, using XRF and wet chemistry. ††Three samples from locality 15, analysed by Classic Comlabs, Adelaide, using XRF and wet chemistry. PGE values for three samples from locality 15, by courtesy of M. W. Wallace, R. R. Keays and V. A. Gostin. §§Total Fe as Fe_2O_3 where no FeO value given. ***Pd, Pt, Au, Ir and Ru values by courtesy of R. R. Keays, M. W. Wallace and V. A. Gostin; analysed by fire assay and neutron activation (see also Gostin et al. 1989).

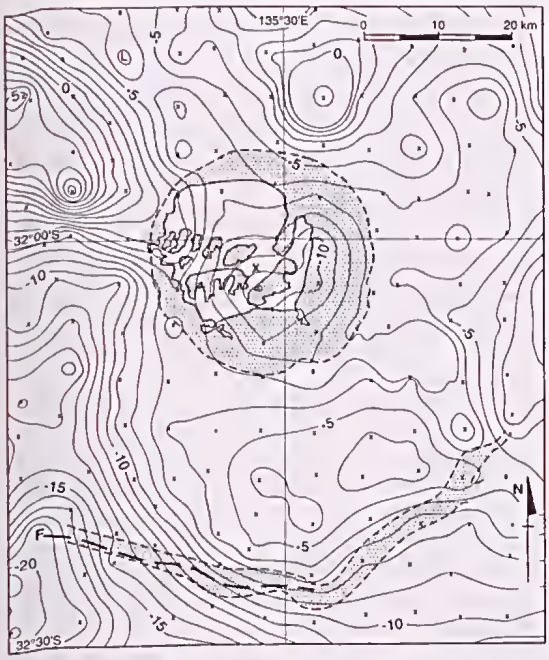

Fig. 10. Bouguer gravity anomaly map of the Gawler Ranges region, showing a negative anomaly centred on the Acraman depression (stippled, except for Lake Acraman). The partly fault-controlled Yardea corridor (stippled, F marks fault) in the south appears unrelated to the gravity signature. Contour interval 1 mGal. L = gravity low. Small crosses mark gravity stations. The large cross in Lake Acraman marks the position of the dipolar aeromagnetic anomaly in the central area (Fig. 11). Recontoured from gravity readings taken by the South Australian Department of Mines and Energy (cf. Yardea and Gairdner 1:250 000 Bouguer Anomaly Maps, South Australian Department of Mines and Energy, Adelaide, 1972).

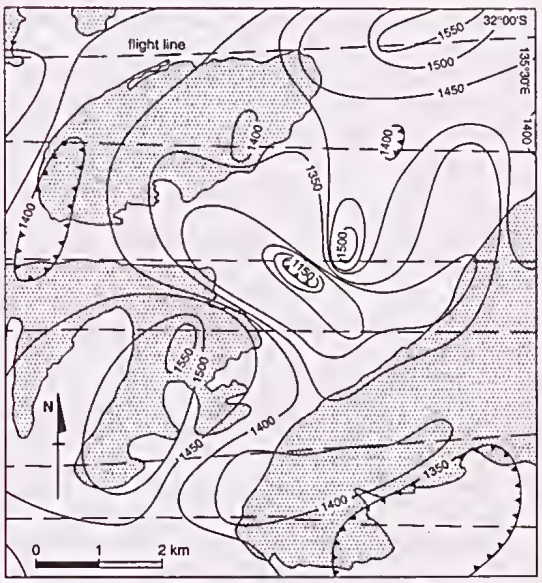

Fig. 11. Aeromagnetic map for the central area of the Acraman structure, showing a dipolar magnetic anomaly between islands (stippled) in Lake Acraman (cf. Fig. 3). The anomaly indicates a shallow magnetic source. Total magnetic intensity was recorded continuously at an altitude of 152 m along the flight lines shown. Contour interval 50 gammas. Modified from Hiltaba 1:63 360 Aeromagnetic Map of Total Intensity, South Australian Department of Mines and Energy, Adelaide, 1961.

Aeromagnetics

The most common magnetic signature associated with impact structures is a magnetic low with subdued magnetic relief caused by a reduction in susceptibility; numerous structures also exhibit a central high-amplitude anomaly (Pilkington & Grieve 1992). High-resolution digital aeromagnetic data (400 m line spacing, 80 m ground clearance) for the Gawler Craton, released by the South Australian Department of Mines and Energy in December 1993, show that Acraman is marked by a circular magnetic low as much as 30 km in diameter exhibiting subdued magnetic relief and a central high-amplitude dipolar anomaly. The magnetic low and subdued magnetic relief are most conspicuous for the innermost 20 km diameter, and the full extent of the subdued signature approximates the limits of the Acraman depression and the presumed present extent of fractured Yardea Dacite. The central anomaly (Fig. 11) is at least +200/−150 gammas in amplitude and indicates a shallow (~300 m depth) magnetic source. The data also indicate the presence of northwest- and northeast-trending faults along the line of the Yardea corridor to the south of the area of subdued magnetic signature.

Specimens of fractured dacite from within the Acraman depression on average show a 70% decrease in magnetic susceptibility compared with those of undisturbed Yardea Dacite; this observation suggests that the subdued magnetic signature at Acraman indeed reflects a decrease in susceptibility. The melt rock has a mean magnetic susceptibility nearly twice that of undisturbed Yardea Dacite.

The presence of the circular magnetic low with subdued magnetic relief and the reduced magnetic susceptibility of the shattered dacite strongly support an impact origin for Acraman. Furthermore, the central anomaly at Acraman equates with the central high-amplitude magnetic anomaly displayed

by many impact structures, including all those >40 km in diameter (see Pilkington & Grieve 1992). The central anomaly at Acraman may reflect basic igneous rocks brought from great depth by structural uplift (see following), or a concentration of melt rock or melt-bearing breccia. The lack of other aeromagnetic anomalies at Acraman attributable to the edges of a melt sheet suggests, however, that melt material in general is not widely distributed.

PALAEOMAGNETISM

Palaeomagnetic study of the Acraman structure (Schmidt & Williams 1991) aimed to constrain the age of the impact and test the postulated correlation of the Acraman impact and deposition of the ejecta horizon in the Bunyeroo Formation in the Adelaide Geosyncline.

Samples for palaeomagnetic analysis comprised shattered dacite (locs 3, 12) and melt rock (loc. 15) from the central area, and undisturbed dacite from as far as 20 km south of the Acraman depression. Only the melt rock responded to magnetic cleaning, and carried a remanent magnetisation that was stable to 630°C. This observation, the coercivity of remanence, and XRD and microprobe analyses indicate that the magnetic carrier is partially oxidised titanomagnetite. That carrier is likely to have retained an original magnetic direction from the time of the impact.

The directions of the high-temperature components from eight prepared specimens of melt rock, and their mean direction and error circle (declination = 48.3°, inclination $I = 54.7°$, $\alpha_{95} = 5.2°$) yield a mean pole position at 8.6°S latitude and 353.4°E longitude ($A_{95} = 6.3°$). The character of the melt-rock remanence, such as low directional dispersion and high stability, is similar to that displayed by impactites containing melt material from other impact structures (e.g. Larochelle & Currie 1967; Pohl 1971; Pohl & Soffel 1971).

The direction of magnetisation of the melt rock is unlike the palaeomagnetic direction found in the Gawler Range Volcanics (see Chamalaun & Dempsey 1978). Furthermore, there is no sign of a present field direction attributable to weathering, or viscous remanent magnetisation (although a lightning-induced component may have obliterated the latter). It is thus concluded that the high-temperature component of the magnetisation dates from the time of cooling immediately after the impact. The indicated pole for the melt rock must be considered a virtual geomagnetic pole (VGP) because the geomagnetic field direction recorded at the time of cooling is an instantaneous sample of a geomagnetic field direction subject to secular variation.

The Neoproterozoic Bunyeroo Formation containing the ejecta horizon is a fine-grained red shale of marine-shelf origin, ideal for palaeomagnetic analysis. The direction of the cleaned magnetisation component of the Bunyeroo Formation was acquired prior to folding of the formation during the Cambro-Ordovician Delamerian Orogeny (McWilliams & McElhinny 1980), which is evidence that its remanence may be original and date from about the time the strata were deposited. The presence of both normal and reverse magnetisations within the Bunyeroo Formation further suggests that the magnetisation is primary, because most overprints are of a single polarity. Indeed, the Bunyeroo palaeomagnetic data satisfy six of the seven 'reliability criteria' for palaeomagnetic data, including a field test, given by Van der Voo (1990).

The pole for the Bunyeroo Formation (McWilliams & McElhinny 1980) is at 7°S latitude and 17°E longitude ($I = -40°$, $A_{95} = 12°$), and may be considered a palaeomagnetic pole (*sensu stricto*) at about the time of deposition. As shown in Fig. 12, this pole is very close to the VGP for the Acraman melt rock, and is quite distinct from probable Delamerian overprint poles for ~450 Ma.

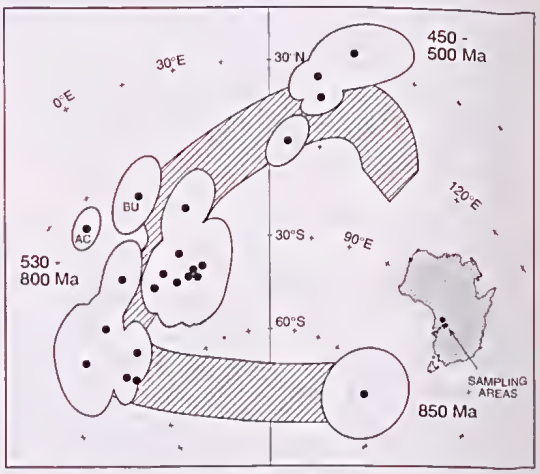

Fig. 12. Pole path (striped) for the Adelaide Geosyncline Gawler–Craton region of South Australia for the interval 850–450 Ma. Solid dots are palaeomagnetic poles mostly determined for strata in the Adelaide Geosyncline (shown with polar error ellipses of 95% confidence). BU, palaeomagnetic pole for the Bunyeroo Formation; AC, virtual geomagnetic pole for melt rock from Acraman. Modified from McWilliams & McElhinny (1980) with additional data from Schmidt & Williams (1991).

Statistical tests show that the Acraman VGP may be regarded as a subset of the Bunycroo palaeomagnetic pole position (Schmidt & Williams 1991), indicating that the two pole positions are statistically indistinguishable. This agreement strongly supports the postulate that the ejecta horizon in the Bunyeroo Formation was derived from Acraman.

The Acraman VGP indicates an instantaneous palaeomagnetic latitude of $35.2 \pm 6.3°$, and the Bunycroo palaeomagnetic pole a palaeolatitude of $22.8 \pm 12.0°$. These data imply that the Acraman impact occurred in low to moderate palaeolatitudes.

GEOCHRONOLOGY

K/Ar and $^{40}Ar/^{39}Ar$ analysis

Conventional K/Ar and $^{40}Ar/^{39}Ar$ total fusion and step heat experiments were performed on two samples of melt rock from locality 15 in an attempt to directly determine the age of the impact (Baldwin et al. 1991). The samples were typical of the melt rock, consisting mainly of albite laths in a devitrified matrix of cloudy K-feldspar and quartz.

An estimate of the apparent age of the melt rock is ~450 Ma, Late Ordovician. Because the feldspars in the melt rock evidently formed as a result of low-temperature authigenic replacement and devitrification, the apparent age is regarded as a *minimum* age for the impact. The apparent age therefore may record the time elapsed since formation of the low-temperature feldspar phases. It may be concluded that the apparent age of ~450 Ma reflects secondary processes rather than the impact event itself.

It is noteworthy that eight K/Ar apparent ages determined for melt rock from the Brent impact structure in Canada averaged only 342 Ma (range 301–414 Ma), much less than the inferred stratigraphic age of 450–500 Ma (Hartung et al. 1971); the melt rock apparent ages for Brent were regarded as minima because of some argon loss subsequent to the impact. The findings for Acraman and Brent indicate that K/Ar and $^{40}Ar/^{39}Ar$ ages for melt rock from degraded, very old (particularly Precambrian) impact structures should be interpreted with caution because the rock dated probably would be exhumed (former depths ≥ 2 km) and may have undergone diagenetic changes such as authigenic replacement of fine-grained feldspars and devitrification of glass.

Apatite fission track analysis

One sample of melt rock (3 kg) and one of shattered Yardea Dacite (4 kg) from localities 15 and 3, respectively, in the central area of Acraman were examined by I. R. Duddy (Geotrack International, Melbourne) for possible fission track dating of zircon, sphene and apatite in an attempt to constrain the age of the Acraman impact. Neither sample yielded sufficient grains of zircon or sphene for reliable fission track analysis, and no apatite was obtained from the melt rock. Sufficient apatite grains for fission track analysis were, however, obtained from the shattered dacite, although the grains were very shattered.

An apatite fission track apparent age of 319 ± 19 Ma is indicated for shattered Yardea Dacite from locality 3 (Table 3). The apparent age agrees with other apatite fission track apparent ages determined by Ferguson (1981) for the Gawler Craton in South Australia (mean of 13 ages = 331 ± 30 Ma, 1σ).

A first-order interpretation of the apatite fission track apparent age is that the sample was at a temperature of $100 \pm 20°C$, the apatite track retention temperature (Moore et al. 1986), at ~320 Ma. The unimodal, negatively skewed distribution of fission track lengths for apatite from the shattered dacite (Fig. 13) is characteristic of areas that have had a steady 'slow-cooling' type of thermal history (see Gleadow et al. 1986). Assuming the apparent age reflects a 'slow-cooling' history, the amount of erosion since 320 Ma could, in principle, be estimated if the palaeogeothermal gradient were known. Conversely, if the maximum amount of erosion since that time were known it would be possible to estimate a minimum palaeogeothermal gradient.

Sample	Number of grains	Spontaneous track density ($\times 10^6$ cm^{-2})	Induced track density ($\times 10^6$ cm^{-2})	Correlation coefficient	Apparent age ± 1σ (Ma)
WAC-3/1	21	1.731 (811)*	1.076 (504)*	0.873	319 ± 19

Table 3. Apatite fission track analytical results for shattered Yardea Dacite, locality 3, central Acraman structure. Data by courtesy of I. R. Duddy, Geotrack International, Melbourne. *Number of tracks counted shown in brackets.

Taking the apatite track retention temperature to be 100±20°C, a mean surface palaeotemperature of 20°C and a 'normal' palaeogeothermal gradient in the range 20–30°C/km (the average geothermal gradient determined for the Gawler Craton is 20–25°C/km; Cull & Conley 1983), the slow-cooling interpretation of the apparent age would seem to require erosion of 2–5 km since 320 Ma. Alternatively, a higher geothermal gradient may have affected the Gawler Craton during the mid-Carboniferous, when the apatite 'clock' was reset at shallower depth. Independent evidence for rates of erosion on the Gawler Craton, or for a regional thermal event during the late Palaeozoic, would be required to discriminate between these two interpretations. In view of evidence for widespread orogenic and thermal activity in central Australia and South Australia during the late Palaeozoic (e.g. Li et al. 1989; Camacho et al. 1991; Idnurm & Heinrich 1993), which may have produced an above-normal palaeogeothermal gradient (≥30°C/km) for the Gawler Craton, the apatite fission track data are perhaps best regarded as indicating a *maximum* of ~2 km of erosion at Acraman since 320 Ma.

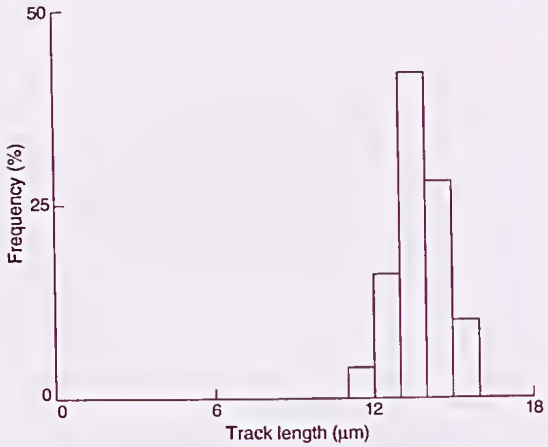

Fig. 13. Frequency histogram of fission track lengths in apatite for shattered Yardea Dacite, locality 3, central Acraman structure. Mean track length, 13.78±0.15 μm; standard deviation of distribution, 1.04 μm; skewness, −0.203; kurtosis, 2.944; number of tracks measured, 50. Data courtesy of I. R. Duddy (Geotrack International, Melbourne).

DISCUSSION – THE ACRAMAN IMPACT EVENT

Evidence for an impact origin of the Acraman structure

Acraman displays numerous criteria for the identification of impact structures (Table 4). Indeed, the Acraman structure qualifies on all criteria given by Dence (1972) for the identification of terrestrial

Criterion (after Dence 1972; Pilkington and Grieve 1992)	Acraman structure
1. Presence of meteorites: rare except in ejecta of *young* craters.	Distal, shocked ejecta with Ir anomaly preserved in Neoproterozoic strata.
2. Circular plan, particularly near centre.	Circular inner topographic depression 30 km in diameter.
3. Rim structure, including disturbed zone or peripheral trough, in complex craters.	Apparent ring structures at 85–90 km and ~150 km diameter.
4. Central structure, with central uplift in complex craters.	'Single peak' central uplift area ≥10 km diameter.
5. Generally negative gravity anomaly.	~6 mGal negative gravity anomaly 30–35 km across associated with the inner topographic depression.
6. Magnetic field variable, commonly subdued. Central magnetic anomaly.	Subdued aeromagnetic signature over inner topographic depression. Dipolar aeromagnetic anomaly in central area.
7. Crater rocks show lower seismic velocities than surrounding rocks.	Seismic data not available.
8. Brecciation observed in outcrop and subsurface.	Rocks of central uplift area intensely shattered and brecciated.
9. Shock metamorphism indicated by shatter cones, shock lamellae in minerals, melt rock, mixed breccias, high-pressure phases.	Shatter cones, multiple sets of shock lamellae in quartz and feldspar grains, melt rock, mixed melt rock and breccia, present in central uplift area.

Table 4. Criteria for the identification of impact structures compared with features displayed by the Acraman structure.

impact structures (excluding young craters) except for his criterion no. 7 (low seismic velocities), seismic data not being available. In addition, Acraman is notable among known terrestrial impact structures in evidently having part of its distal ejecta blanket of rock fragments preserved (Gostin et al. 1986; Compston et al. 1987; Wallace et al. 1989, 1990c). This ejecta horizon is anomalous in cosmogenic siderophile elements, including Ir (Gostin et al. 1989; Wallace et al. 1990b, 1990c), and locally contains abundant altered tektite-like spherules and shard-like clasts (Wallace et al. 1990a). These observations together leave no reasonable doubt that the Acraman structure is of impact origin.

Age of the impact

Dating techniques have not provided a direct estimate of the age of the Acraman impact. The most that can be concluded, from the K/Ar and $^{40}Ar/^{39}Ar$ data, is that the impact occurred *at least* 450 million years ago. The likely age of the impact is, however, provided by stratigraphy. Much data together argue strongly that Acraman is the source of the ejecta horizon near the base the Neoproterozoic Bunyeroo Formation in the Adelaide Geosyncline and the correlative Rodda Beds in the Officer Basin (Gostin et al. 1986, 1989; Wallace et al. 1989, 1990c):

1. All large fragments (pebble to boulder size) and sand-grade clastic material in the ejecta were derived from pink to red felsic volcanic rocks similar to the Yardea Dacite at Acraman.

2. Comparable shattering and shock pressures (up to ~15 GPa) are displayed by ejecta clasts and shattered Yardea Dacite in the central area at Acraman.

3. Shattered euhedral zircons from ejecta clasts gave a U-Pb age of 1575±11 Ma (Compston et al. 1987), which is nearly concordant with the U-Pb zircon age of 1592±3 Ma for the Yardea Dacite (Fanning et al. 1988). The slightly younger age for the ejecta may indicate derivation of material from a higher stratigraphic level than that of the dacite now exposed at the impact site, or possible lead loss due to shock resetting.

4. The geographic distribution of the preserved ejecta horizon (Fig. 14) and the regional variation of ejecta clast size (Wallace et al. 1990c) are consistent with Acraman as the source.

5. Palaeomagnetic data support correlation of the Acraman impact and deposition of the ejecta horizon in the Bunyeroo Formation (Schmidt & Williams 1991).

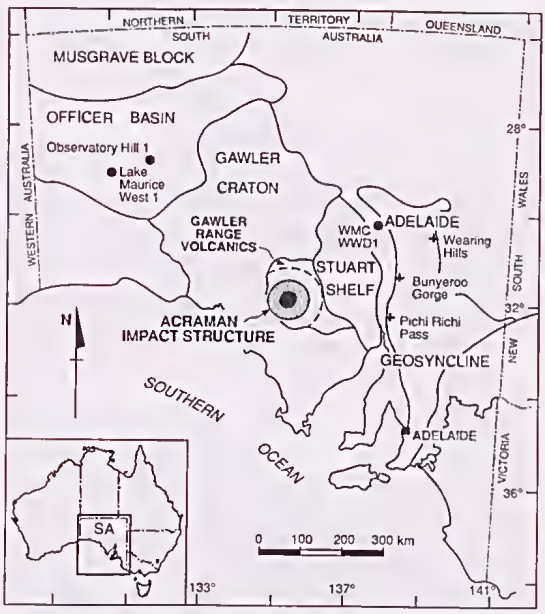

Fig. 14. Map of South Australia showing the Acraman impact structure and the main localities of the related ejecta horizon in the Adelaide Geosyncline and Officer Basin. Crosses indicate ejecta recorded in outcrop of the Bunyeroo Formation, small solid dots ejecta in core from drill holes (see Gostin et al. 1986; Wallace et al. 1989, 1990c).

Hence, determination of the age of the Bunyeroo Formation should provide the age of the Acraman impact. The Yarloo Shale, the equivalent of the Bunyeroo Formation on the Stuart Shelf (Fig. 14), gave a Rb-Sr total rock age of 588±35 Ma (Webb et al. 1983). Combined Rb-Sr total rock data for the Yarloo Shale and subjacent shales gave a mean age of 593±32 Ma (Compston et al. 1987). Thus, the age of the Bunyeroo Formation may be approximated as 590 Ma. A late Neoproterozoic age is consistent with the advanced degradation of Acraman.

The interpretation of such Rb-Sr total rock data is complicated by the possible effects of inherited detrital mica and subsequent diagenesis. According to the Neoproterozoic stratigraphy of Harland et al. (1990, p. 29), the Bunyeroo Formation forms the lowermost unit of the Wonokan Stage of the Ediacara Epoch; Harland et al. (1990) place the base of the Wonokan at 590 Ma, some 20 million years older than their estimate of 570 Ma for the base of the Cambrian. However, recent time-scales incorporating the latest U-Pb zircon ages place the base of the Cambrian at 540 Ma (Odin & Odin

1990; Young & Claoué-Long 1991). Hence, the age of the Bunyeroo Formation and its ejecta horizon may prove to be as young as 560 Ma.

Depth of erosion since the impact

Aeraman displays 'erosional level 7' of Grieve & Robertson (1979), which they define as 'crater floor removed, substructure exposed'. The peak recorded shock pressure of ~15 GPa for bedrock exposed at the centre of Aeraman is lower than the expected 25–30 GPa at the centre of terrestrial complex structures (see Grieve 1988), indicating erosion at Aeraman to a level below the autochthonous crater floor.

The depth of erosion since the impact may be estimated by several methods. The 'slow cooling' interpretation of the apatite fission track data may indicate as much as 2 km of erosion since 320 Ma, assuming an above-normal palaeogeothermal gradient (≥ 30°C/km) for the region in late Palaeozoic time. Such an erosion rate, if projected over the past 600 m.y., would give as much as 4 km of erosion of the Gawler Range Volcanics since the impact.

Rates of erosion in southern Australia over the past 100–200 m.y., if applicable since 600 Ma, suggest a smaller figure for depth of erosion since the impact. The high-level, Cretaceous Nott Surface in the Gawler Ranges, now dissected to depths of 250 m, is an etch surface likely once mantled by a thick regolith; hence, as much as 350 m of erosion may have occurred in parts of the Gawler Ranges region over the past 100 m.y. Taking this erosion rate of 3.5 m/m.y. as the mean rate of Phanerozoic erosion in the Gawler Ranges region—the Gawler Craton may have been severely eroded during its Permian continental glaciation (see Crowell & Frakes 1971)—some 2 km of erosion since the impact would be indicated.

Because the crater has been removed by erosion, an estimate of crater depth would provide a minimum depth of erosion since the impact. From Pilkington & Grieve (1992), true final depth d_f (from crater rim to base of crater fill) $= 0.52\ D_f^{0.2}$, where D_f is the final crater diameter for crystalline targets. Taking the diameter of the Acraman depression of 30 km as a minimum final crater diameter (as discussed below, the final rim-to-rim diameter may have been greater) gives $d_f =$ 1.03 km. Thus, at least 1 km of erosion has occurred since the impact.

Hence, 2 km of erosion and perhaps up to twice that figure may have occurred at Aeraman since the impact at ~590 Ma. By comparison, 1.5 to 2 km of erosion probably has occurred near the centre of the Siljan structure in Sweden since the impact at 368 Ma (Grieve 1988, 1991), indicating an erosion rate at Siljan closer to the lower estimate for Aeraman.

Dimensions and structure of the former crater

The dimensions of the former crater at Acraman must be estimated from the extent of disturbed rocks as much as a kilometre or more below the crater floor. Such estimates must be made with caution, for as noted by Grieve (1991), erosional processes on the Earth can enhance, modify or remove original morphological elements of an impact structure.

The diameter of the Aeraman depression, which evidently is underlain by fractured rocks, provides a guide to the diameters of the transient cavity and excavated area. However, the relation among shock-wave attenuation rates with depth, the diameters of the transient cavity and excavated area, and the approximate limit of disrupted bedrock varies according to the size of the impactor and the energy of the impact (Dence et al. 1977). Applying the three models of Dence et al. (1977, their fig. 10) to Aeraman, the diameters of the transient cavity and excavated area could be as much as 30% greater than the horizontal limits of disrupted bedrock (2 GPa) at the level for 15 GPa central shock-pressure (the maximum shock pressure observed for bedrock outcrop at the centre of Aeraman), the estimated adjustment factor depending on the energy of the impact. A minimum diameter of 3.0×10^4 m for the transient cavity/excavated area at Aeraman gives an energy $\geq 10^{22}$ J (from Dence et al. 1977), suggesting that an adjustment factor of 30% for cavity diameter may apply. Hence, the transient cavity and excavated area at Aeraman may have been as great as 40 km in diameter, 30% greater than the diameter of the Acraman depression. This figure is consistent with the estimate (Grieve 1988) that erosion has reduced the apparent diameter of the excavated area at Siljan, Sweden, by 12–15% for a depth of erosion perhaps only about half that at Aeraman.

According to Grieve (1991), the depth of excavation of the transient cavity $d_c \approx 0.1\ D_t$, where D_t is the diameter of the transient cavity. Taking $D_t = 40$ km for Acraman gives a depth of excavation of ~4 km. Such a depth of excavation is allowable given the present thickness of ~4 km for the Gawler Range Volcanics estimated from gravity data and the possible erosion of 2 km or more of volcanics since the impact.

The centre of the Aeraman depression is marked by a dipolar aeromagnetic anomaly, sparse out-

crops of intensely shattered and shock-deformed Yardea Dacite, and an apparent dyke of fine-grained, generally inclusion-poor melt rock. This central area is interpreted as the central uplift, with a diameter ≥ 10 km. According to Melosh (1989), the central uplift of an impact structure forms by wholesale collapse of an initially deep transient cavity, mainly by uplift of rocks below the crater's centre while rim rocks slump downward and inward.

The apparent lack of bounding faults near the margin of the Acraman depression suggests that the final structural rim occurred at a greater diameter. Possibly the final structural rim is marked by the partly fault-controlled ring at 85–90 km diameter; the polygonal shape of this ring feature implies that any final collapse occurred along pre-existing fractures. According to Grieve (1987, 1991), the diameter of obvious excavation of a terrestrial impact structure $D_e = 0.50–0.65\ D_f$, and Lakomy (1990) gives the transient cavity diameter $D_t = (0.57 \pm 0.03)D_f$ for seven Phanerozoic impact structures. Figures for the Sudbury structure ($D_t \approx 100$ km and $D_f \approx 150–200$ km; Grieve et al. 1991) are in the ratio 0.50–0.67. The estimates of D_t and $D_e = 40$ km for Acraman and the diameter of the apparent ring at 85–90 km are in the ratio 0.44–0.47; this range approaches the lower limit for other structures, despite the severe degradation of Acraman and the evident influence of prior structure on the location of the ring feature at 85–90 km diameter.

Available data suggest that the pre-erosional form of Acraman was that of a 'central peak crater' (see Melosh 1989). Diameters of the uneroded structural features—central uplift, excavated area, and possible final structural rim—may have been ≥ 10 km, ~40 km, and 85–90 km, respectively. Interestingly, these dimensions are comparable to those of numerous 'protobasins' (large peak plus inner-ring basins) on Mercury and Mars (see Pike & Spudis 1987). A diameter D_f of 85–90 km for the final structural rim would indicate a true depth d_f of 1.3 km after slumping of the crater walls (see Pilkington & Grieve 1992). Arcuate features at ~150 km diameter may be faults or fractures marking the outer limit of disturbance. It is noteworthy that the Manicouagan impact structure in Quebec likewise has an outer topographic ring at ~150 km diameter which may mark the outer limit of disturbance well beyond the final structural rim at 100 km diameter (Dence 1977; Grieve & Head 1983).

Grieve (1991) suggested that $SU = 0.06\ D_f^{1.1}$, where SU is the observed amount of uplift undergone by the deepest horizon now exposed in the central uplift of a complex structure. According to Pilkington & Grieve (1992), SU also may provide a useful estimate of the depth of the fractured zone. For Acraman, taking $D_f = 85–90$ km gives SU = 8.0–8.5 km. This figure suggests that dense basic rocks presumed from gravity data to underlie the Gawler Range Volcanics at a depth between ~4–12 km may now be near the surface in the central uplift. The dipolar magnetic anomaly over the central uplift is consistent with the presence of basic rocks or melt rock at shallow depth. Drilling would be required to determine the source of this anomaly.

Dynamics of the impact

The relationship for crater diameter as a function of impactor diameter and velocity (Schmidt & Holsapple 1982, their fig. 6) indicates that a transient cavity/excavated area 40 km in diameter, as estimated here for Acraman, could have been formed by an impactor 5.5 km in diameter and density 2200 kg/m^3 travelling at 25 km/s. As the geochemistry of the Bunyeroo ejecta layer suggests that the Acraman impactor had a chondritic composition (Gostin et al. 1989; Wallace et al. 1990c), a density of 3500 kg/m^3 is more appropriate, giving an impactor diameter of 4.7 km for a velocity of 25 km/s.

These figures indicate that the Acraman impactor had kinetic energy of 6×10^{22} J, which was converted to explosive energy (equivalent to 1.5×10^7 megatons) on impact. By comparison, the 1-km-diameter Meteor Crater in Arizona had a formation energy ≤ 60 megatons and the largest man-made nuclear detonation was 60 megatons (Melosh 1989).

Acraman shows some evidence of asymmetry in plan. The deepest part of the regional negative gravity anomaly (Fig. 10), the dipolar magnetic anomaly (Fig. 11) and the area of shattered rocks marking the central uplift appear offset 1–2 km south of the centre of the Acraman depression (Fig. 3). Furthermore, the 85–90-km ring structure is most clearly expressed in the south as the fault-controlled Yardea corridor (Figs 1, 2 and 10). Because complex craters produced by oblique impact may exhibit an uprange offset of the central peak complex and more extensive rim/wall collapse uprange (Schultz & Gault 1992), the observations for Acraman may suggest oblique impact from the south (south uprange).

Ejecta blanket

The sedimentology, geochemistry and distribution of preserved ejecta from Acraman are discussed

by Gostin et al. (1986, 1989) and Wallace et al. (1989, 1990a, 1990b, 1990c); the main ejecta localities are shown in Fig. 14. The thickness of the ejecta layer in the Adelaide Geosyncline 220–350 km east of Acraman ranges from 0–400 mm, with clasts as much as 300 mm in diameter. Distances given are minima for the time of impact because subsequent folding and reverse faulting within the Geosyncline would have shortened the distances between impact and eastern ejecta sites, possibly by tens of kilometres (Gostin et al. 1986). The sandy ejecta in the Officer Basin 470 km northwest of the impact site, seen only in two drill cores, is <1 mm to 7 mm thick. True thicknesses of ejecta that fell in the Adelaide Geosyncline may be less than maximum recorded thicknesses because of likely resedimentation of ejecta material (see Gostin et al. 1986). The formation of ejecta rays also could cause lateral variation in ejecta thickness. Study of ejecta distribution in the Bunyeroo Formation and Rodda Beds may test the suggestion of oblique impact from the south, although relatively few good exposures of the Bunyeroo Formation are known in the southern Adelaide Geosyncline.

Cratering data (obtained from small-scale laboratory experiments, nuclear and high-explosive craters, terrestrial meteorite impact craters, and estimates for lunar craters) suggest that, over a wide range of scales, ejecta blanket thickness t decreases with distance r from a crater centre as

$$t = 0.14R^{0.74}(r/R)^{-3.0} \text{ for } r \geqslant R \qquad (1)$$

where R is the transient crater radius and all dimensions are in metres (McGetchin et al. 1973). Employing Equation (1), a transient crater radius of 2×10^4 m for Acraman gives a thickness for undisturbed ejecta of 160 mm at a distance of 220 km from the crater centre, a thickness of 40 mm at a radius of 350 km, and a thickness of 16 mm at a radius of 470 km. These estimated thicknesses for an undisturbed ejecta blanket are of the same order as observed thicknesses for the ejecta horizons in the Bunyeroo Formation and Rodda Beds.

At a radius of 470 km, the Acraman ejecta of rock fragments, sand and glassy material would have covered 6.9×10^5 km^2, nearly three times the area of the United Kingdom. Finer-grained ejecta and dust would have spread much farther, and consequences of the impact could have exerted medium-term (days to months) influence on global climate. McLaren & Goodfellow (1990) concluded that evidence should be sought for an influence of the Acraman impact event on Vendian (late Neoproterozoic) biota and geochemistry.

As observed by Gostin et al. (1989), the unique character of the ejecta derived from Acraman may permit intercontinental correlation of Neoproterozoic sediments. Young (1992) suggested that the most convincing support for the hypothesis that Australia and North America were juxtaposed during the Neoproterozoic would be the discovery of the Acraman ejecta in strata of the northern Canadian Cordillera. The continental reconstruction of Young (1992, his fig. 1) implies that Neoproterozoic deposition in the Canadian Cordillera occurred within 800–1000 km of the Acraman impact site. Taking the transient crater radius for Acraman as 2×10^4 m, Equation (1) indicates that the thickness of an undisturbed ejecta layer would be 3.3 mm at 800 km radius and 1.7 mm at 1000 km. Such potential thicknesses and possible identifiable trace element and rare-earth element geochemical fingerprints of ejecta derived from the Gawler Range Volcanics (see Table 2 and Fig. 9) together may provide a tangible target in any search for the Acraman ejecta horizon within Neoproterozoic shales in the Canadian Cordillera.

EARTH'S CRATERING RECORD

Some 130 terrestrial impact craters and structures are currently recognised, nine of which are >50 km in diameter (Grieve 1991). Acraman could have resulted from impact with a large, Earth-crossing asteroid, there presently being an estimated 2000 such bodies $\geqslant1$ km in diameter (Ahrens & Harris 1992; Matthews 1992; Shoemaker 1992). According to Shoemaker, the Earth-crossing swarm 'is depleted by collision of some of these asteroids with the planets and by ejection of others from the solar system. The swarm is replenished chiefly by collisional fragmentation of main-belt asteroids and injection of the fragments into Earth-crossing orbits.'

In the present regime, an asteroid >1 km in diameter strikes the Earth and produces a crater >10 km in diameter about once every 100 000 years, on average. An Acraman-sized impact with an Earth-crossing asteroid occurs on average every few tens of millions of years. The Earth also resides in a swarm of comets, members of which also occasionally strike our planet. A comet nucleus >10 km in diameter collides with the Earth and produces a crater >150 km in diameter about once every 100 million years, on average.

As stressed by Shoemaker (1992), impact of asteroids and comets is a *normal geological process* that has persisted throughout Earth history. It is being increasingly acknowledged that this process has had a major influence on the development

of life, at least during the Phanerozoic. Indeed, were it not for the active processes of erosion that have long existed on the Earth and which remove traces of all but the largest impacts in less than 600 million years, our planet would be as pock-marked with impact craters as are the other terrestrial planets.

ACKNOWLEDGEMENTS

I thank Vic Gostin, Malcolm Wallace and Reid Keays for discussion and providing some geochemical data for rocks from Acraman, Phil Schmidt for palaeomagnetic analysis of melt rock, Sue Baldwin and Ian McDougall for K/Ar and $^{40}Ar/^{39}Ar$ analysis of melt rock, Ian Duddy for providing apatite fission track data for shattered dacite, Zhiqun Shi and David Boyd for discussion of geophysical data, Huw Rosser for assistance with electron probe analysis, and Sherry Proferes for drafting. The Australian Surveying and Land Information Group, Canberra, gave permission to reproduce digital elevation images, and BHP Minerals Exploration Department, Melbourne, processed certain digital images and agreed to their publication. The work is supported by the Australian Research Council.

REFERENCES

Ahrens, T. J. & Harris, A. W., 1992. Deflection and fragmentation of near-Earth asteroids. *Nature* 360: 429–433.

Baldwin, S. L., McDougall, I. & Williams, G. E., 1991. K/Ar and $^{40}Ar/^{39}Ar$ analyses of meltrock from the Acraman impact structure, Gawler Ranges, South Australia. *Australian Journal of Earth Sciences* 38: 291–298.

Blissett, A. H., 1977. Gairdner map sheet, 1:250 000 Geological Series. South Australian Department of Mines and Energy, Adelaide.

Blissett, A. H., 1986. Subdivision of the Gawler Range Volcanics in the Gawler Ranges. *Geological Survey of South Australia Quarterly Geological Notes* 97: 2–11.

Blissett, A. H. (comp.), 1987. Geological setting of the Gawler Range Volcanics, Geological Atlas Special Series, 1:500 000. South Australian Department of Mines and Energy, Adelaide.

Blissett, A. H., Parker, A. J. & Crooks, A. F., 1988. Yardea map sheet, 1:250 000 Geological Series. South Australian Department of Mines and Energy, Adelaide.

Blissett, A. H., Parker, A. J. & Scheffler, J., 1989. Gawler Ranges excursion, October 7th–9th, 1989. *South Australian Department of Mines and Energy Report Book* 89/70, 47 p.

Boles, J. R., 1982. Active albitization of plagioclase, Gulf Coast Tertiary. *American Journal of Science* 282: 165–180.

Bowler, J. M., 1986. Spatial variability and hydrologic evolution of Australian lake basins: analogue for Pleistocene hydrologic change and evaporite formation. *Palaeogeography, Palaeoclimatology, Palaeoecology* 54: 21–41.

Branch, C. D., 1978. Evolution of the Middle Proterozoic Chandabooka Caldera, Gawler Range acid volcano-plutonic province, South Australia. *Journal of the Geological Society of Australia* 25: 199–216.

Camacho, A., Simons, B. & Schmidt, P. W., 1991. Geological and palaeomagnetic significance of the Kulgera Dyke Swarm, Musgrave Block, NT, Australia. *Geophysical Journal International* 107: 37–45.

Campbell, E. M. & Twidale, C. R., 1991. The evolution of bornhardts in silicic volcanic rocks in the Gawler Ranges. *Australian Journal of Earth Sciences* 38: 79–93.

Carmichael, I. S. E., Turner, F. J. & Verhoogen, J., 1974. *Igneous Petrology*. McGraw-Hill, New York, 739 p.

Chamalaun, F. H. & Dempsey, C. E., 1978. Palaeomagnetism of the Gawler Range Volcanics and implications for the genesis of the Middlebaek hematite orebodies. *Journal of the Geological Society of Australia* 25: 255–265.

Compston, W., Williams, I. S., Jenkins, R. J. F., Gostin, V. A. & Haines, P. W., 1987. Zircon age evidence for the Late Precambrian Acraman ejecta blanket. *Australian Journal of Earth Sciences* 34: 435–445.

Crawford, A. R., 1963. Large ring structures in a South Australian Precambrian volcanic complex. *Nature* 197: 140–142.

Creaser, R. A., 1989. The Geology and Petrology of Middle Proterozoic Felsic Magmatism of the Stuart Shelf, South Australia. La Trobe University, Melbourne, PhD thesis (unpubl.).

Creaser, R. A. & White, A. J. R., 1991. Yardea Dacite —large-volume, high-temperature felsic volcanism from the Middle Proterozoic of South Australia. *Geology* 19: 48–51.

Crowell, J. C. & Frakes, L. A., 1971. Late Paleozoic glaciation: Part IV, Australia. *Geological Society of America Bulletin* 82: 2515–2540.

Cull, J. P. & Conley, D., 1983. Geothermal gradients and heat flow in Australian sedimentary basins. *BMR Journal of Australian Geology and Geophysics* 8: 329–337.

Currie, K. L. & Shafiqullah, M., 1968. Geochemistry of some large Canadian craters. *Nature* 218: 457–459.

Dence, M. R., 1971. Impact melts. *Journal of Geophysical Research* 76: 5552–5565.

Dence, M. R., 1972. The nature and significance of terrestrial impact structures. *24th International Geological Congress, Montreal*, Section 15: 77–89.

DENCE, M. R., 1977. The Manicouagan impact structure observed from Skylab. *NASA Report* SP-380: 175–189.

DENCE, M. R., GRIEVE, R. A. F. & ROBERTSON, P. B., 1977. Terrestrial impact structures: principal characteristics and energy considerations. In *Impact and Explosion Cratering*, D. J. Roddy, R. O. Pepin & R. B. Merrill, eds, Pergamon, New York, 247–275.

FANNING, C. M., FLINT, R. B., PARKER, A. J., LUDWIG, K. R. & BLISSETT, A. H., 1988. Refined Proterozoic evolution of the Gawler Craton, South Australia, through U-Pb zircon geochronology. *Precambrian Research* 40/41: 363–386.

FERGUSON, K. U., 1981. Fission Track Dating of Shield Areas, Australia: Relationships Between Tectonic and Thermal Histories and Fission Track Age Distribution. University of Melbourne, MSc thesis, 194 p. (unpubl.).

GILES, C. W., 1977. Rock units in the Gawler Range Volcanics, Lake Everard area, South Australia. *Geological Survey of South Australia Quarterly Geological Notes* 61: 7–16.

GILES, C. W., 1988. Petrogenesis of the Proterozoic Gawler Range Volcanics, South Australia: *Precambrian Research* 40/41: 407–427.

GLEADOW, A. J. W., DUDDY, I. R., GREEN, P. F. & HEGARTY, K. A., 1986. Fission track lengths in the apatite annealing zone and the interpretation of mixed ages. *Earth and Planetary Science Letters* 78: 245–254.

GOSTIN, V. A., HAINES, P. W., JENKINS, R. J. F., COMPSTON, W. & WILLIAMS, I. S., 1986. Impact ejecta horizon within late Precambrian shales, Adelaide Geosyncline, South Australia. *Science* 233: 198–200.

GOSTIN, V. A., KEAYS, R. R. & WALLACE, M. W., 1989. Iridium anomaly from the Acraman impact ejecta horizon: impacts can produce sedimentary iridium peaks. *Nature* 340: 542–544.

GRIEVE, R. A. F., 1987. Terrestrial impact structures. *Annual Review of Earth and Planetary Sciences* 15: 245–270.

GRIEVE, R. A. F., 1988. The formation of large impact structures and constraints on the nature of Siljan. In *Deep Drilling in Crystalline Bedrock, Volume I: The Deep Gas Drilling in the Siljan Impact Structure, Sweden and Astroblemes*, A. Bodén & K. G. Eriksson, eds, Springer, Berlin, 328–348.

GRIEVE, R. A. F., 1991. Terrestrial impact: the record in the rocks. *Meteoritics* 26: 175–194.

GRIEVE, R. A. F., DENCE, M. R. & ROBERTSON, P. B., 1977. Cratering processes: as interpreted from the occurrence of impact melts. In *Impact and Explosion Cratering*, D. J. Roddy, R. O. Pepin & R. B. Merrill, eds, Pergamon, New York, 791–814.

GRIEVE, R. A. F. & HEAD, J. W., 1983. The Manicouagan impact structure: an analysis of its original dimensions and form. *Proceedings of the 13th Lunar and Planetary Science Conference, Journal of Geophysical Research* 88: suppl. A807–A818.

GRIEVE, R. A. F. & ROBERTSON, P. B., 1979. The terrestrial cratering record. I. Current status of observations. *Icarus* 38: 212–229.

GRIEVE, R. A. F., STÖFFLER, D. & DEUTSCH, A., 1991. The Sudbury structure: controversial or misunderstood? *Journal of Geophysical Research* 96: 22 753–22 764.

HARLAND, W. B., ARMSTRONG, R. L., COX, A. V., CRAIG, L. E., SMITH, A. G. & SMITH, D. G. (eds), 1990. *A Geologic Time Scale 1989*. Cambridge University Press, Cambridge, 263 p.

HARTUNG, J. B., DENCE, M. R. & ADAMS, J. A. S., 1971. Potassium-argon dating of shock-metamorphosed rocks from the Brent impact crater, Ontario, Canada. *Journal of Geophysical Research* 76: 5437–5448.

IDNURM, M. & HEINRICH, C. A., 1993. A palaeomagnetic study of hydrothermal activity and uranium mineralization at Mt Painter, South Australia. *Australian Journal of Earth Sciences* 40: 87–101.

JOHNS, R. K., 1968. Investigation of lakes Torrens and Gairdner. *South Australian Department of Mines Report of Investigations* 31, 90 p.

KASTNER, M. & SIEVER, R., 1979. Low temperature feldspars in sedimentary rocks. *American Journal of Science* 279: 435–479.

LAKOMY, R., 1990. Distribution of impact induced phenomena in complex terrestrial impact structures: implications for transient cavity dimensions. *Proceedings of the Lunar and Planetary Science Conference* 21: 676–677.

LAROCHELLE, A. & CURRIE, K. L., 1967. Paleomagnetic study of igneous rocks from the Manicouagan structure, Quebec. *Journal of Geophysical Research* 72: 4163–4169.

LEVINSON, A. A., 1974. *Introduction to Exploration Geochemistry*. Applied Publishing, Calgary, 612 p.

LI, Z. X., POWELL, C. MCA. & SCHMIDT, P. W., 1989. Syn-deformational remanent magnetization of the Mount Eclipse Sandstone, central Australia. *Geophysical Journal International* 99: 205–222.

MATTHEWS, R., 1992. A rocky watch for Earthbound asteroids. *Science* 255: 1204–1205.

MCGETCHIN, T. R., SETTLE, M. & HEAD, J. W., 1973. Radial thickness variation in impact crater ejecta: implications for lunar basin deposits. *Earth and Planetary Science Letters* 20: 226–236.

MCLAREN, D. J. & GOODFELLOW, W. D., 1990. Geological and biological consequences of giant impacts. *Annual Review of Earth and Planetary Sciences* 18: 123–171.

MCWILLIAMS, M. O. & MCELHINNY, M. W., 1980. Late Precambrian paleomagnetism of Australia: the Adelaide Geosyncline. *Journal of Geology* 88: 1–26.

MELOSH, H. J., 1989. *Impact Cratering*. Oxford University Press, New York, 245 p.

MILTON, D. J., 1977. Shatter cones—an outstanding problem in shock mechanics. In *Impact and Explosion Cratering*, D. J. Roddy, R. O. Pepin & R. B. Merrill, eds, Pergamon, New York, 703–714.

MOORE, M. E., GLEADOW, A. J. W. & LOVERING, J. F.,

1986. Thermal evolution of rifted continental margins: new evidence from fission tracks in basement apatites from southeastern Australia. *Earth and Planetary Science Letters* 78: 255–270.

Odin, G.-S. & Odin, C., 1990. Échelle numérique des temps géologiques. *Bureau de Recherches Géologiques et Minières, Société Géologique de France*, no. 35.

Palme, H., 1982. Identification of projectiles of large terrestrial impact craters and some implications for the interpretation of Ir-rich Cretaceous/Tertiary boundary layers. *Geological Society of America Special Paper* 190: 223–233.

Parfenova, O. V. & Yakovlev, O. I., 1977. Some peculiarities of selective evaporation in target rocks after meteoritic impact. In *Impact and Explosion Cratering*, D. J. Roddy, R. O. Pepin & R. B. Merrill, eds, Pergamon, New York, 843–859.

Parker, A. J., Rickwood, P. C., Baillie, P. W., McClenaghan, M. P., Boyd, D. M., Freeman, M. J., Pietsch, B. A., Murray, C. G. & Myers, J. S., 1987. Mafic dyke swarms of Australia. In *Mafic Dyke Swarms*, H. C. Halls & W. F. Fahrig, eds, *Geological Association of Canada Special Paper* 34: 401–417.

Pike, R. J. & Spudis, P. D., 1987. Basin-ring spacing on the Moon, Mercury, and Mars. *Earth, Moon, and Planets* 39: 129–194.

Pilkington, M. & Grieve, R. A. F., 1992. The geophysical signature of terrestrial impact structures. *Reviews of Geophysics* 30: 161–181.

Pohl, J., 1971. On the origin of the magnetization of impact breccias on Earth. *Zeitschrift für Geophysik* 37: 549–555.

Pohl, J. & Soffel, H., 1971. Paleomagnetic age determination of the Rochechouart impact structure (France). *Zeitschrift für Geophysik* 37: 857–866.

Robertson, P. B., Dence, M. R. & Vos, M. A., 1968. Deformation in rock-forming minerals from Canadian craters. In *Shock Metamorphism of Natural Materials*, B. M. French & N. M. Short, eds, Mono Book Corporation, Baltimore, 433–452.

Robertson, P. B. & Grieve, R. A. F., 1977. Shock attenuation at terrestrial impact structures. In *Impact and Explosion Cratering*, D. J. Roddy, R. O. Pepin & R. B. Merrill, eds, Pergamon, New York, 687–702.

Rutland, R. W. R., Parker, A. J., Pitt, G. M., Preiss, W. V. & Murrell, B., 1981. The Precambrian of South Australia. In *Precambrian of the Southern Hemisphere*, D. R. Hunter, ed., Elsevier, Amsterdam, 309–360.

Schmidt, P. W. & Williams, G. E., 1991. Palaeomagnetic correlation of the Acraman impact structure and the Late Proterozoic Bunyeroo ejecta horizon, South Australia. *Australian Journal of Earth Sciences* 38: 283–289.

Schmidt, R. M. & Holsapple, K. A., 1982. Estimates of crater size for large-body impact: gravity-scaling results. *Geological Society of America Special Paper* 190: 93–102.

Schultz, P.H. & Gault, D. E., 1992. Recognizing impactor signatures in the planetary record. In *Large Meteorite Impacts and Planetary Evolution: Lunar and Planetary Institute Contribution* 790: 64–65.

Shoemaker, E. M., 1992. Large-body impact is a geologic process. *Geological Society of America Abstracts with Programs* 24: A134.

Solomon, S. C. & Duxbury, E. D., 1987. A test of the longevity of impact-induced faults as preferred sites for later tectonic activity. *Proceedings of the 17th Lunar and Planetary Science Conference, Journal of Geophysical Research* 92 (B4): E759–E768.

Turner, A. R., 1975. The petrology of the eastern Gawler Range Volcanic Complex. *Geological Survey of South Australia Bulletin* 45, 135 p.

Twidale, C. R., Bourne, J. A. & Smith, D. M., 1976. Age and origin of palaeosurfaces on Eyre Peninsula and the southern Gawler Ranges, South Australia. *Zeitschrift für Geomorphologie* 20: 28–55.

Van der Voo, R., 1990. The reliability of paleomagnetic data. *Tectonophysics* 184: 1–9.

Wallace, M. W., Gostin, V. A. & Keays, R. R., 1989. Discovery of the Acraman impact ejecta blanket in the Officer Basin and its stratigraphic significance. *Australian Journal of Earth Sciences* 36: 585–587.

Wallace, M. W., Gostin, V. A. & Keays, R. R., 1990a. Spherules and shard-like clasts from the late Proterozoic Acraman impact ejecta horizon, South Australia. *Meteoritics* 25: 161–165.

Wallace, M. W., Gostin, V. A. & Keays, R. R., 1990b. Acraman impact ejecta and host shales: evidence for low-temperature mobilization of iridium and other platinoids. *Geology* 18: 132–135.

Wallace, M. W., Williams, G. E., Gostin, V. A. & Keays, R. R., 1990c. The Late Proterozoic Acraman impact—towards an understanding of impact events in the sedimentary record. *Mines and Energy Review, South Australia* 57: 29–35.

Webb, A. W., Coats, R. P., Fanning, C. M. & Flint, R. B., 1983. Geochronological framework of the Adelaide Geosyncline. *Geological Society of Australia Abstracts* 10: 7–9.

Williams, G. E., 1986. The Acraman impact structure: source of ejecta in late Precambrian shales, South Australia. *Science* 233: 200–203.

Williams, G. E., 1987. The Acraman structure—Australia's largest impact scar. *Search* 18: 143–145.

Williams, G. E., 1990. The Acraman impact structure, South Australia. *Abstracts for the International Workshop on Meteorite Impact on the Early Earth, Perth, Australia. Lunar and Planetary Institute Contribution* 746: 60–61.

Young, G. & Claoué-Long, J., 1991. Age control on sedimentary sequences. *BMR Research Newsletter* 15: 14–16.

Young, G. M., 1992. Late Proterozoic stratigraphy and the Canada–Australia connection. *Geology* 20: 215–218.